Article

Molecular Spectroscopy of Uranium(IV) Bis(ketimido) Complexes. Rare Observation of Resonance-Enhanced Raman Scattering from Organoactinide Complexes and Evidence for Broken-Symmetry Excited States

Ryan E. Da Re, Kimberly C. Jantunen, Jeffrey T. Golden, Jaqueline L. Kiplinger, and David E. Morris

J. Am. Chem. Soc., **2005**, 127 (2), 682-689• DOI: 10.1021/ja044315g • Publication Date (Web): 17 December 2004

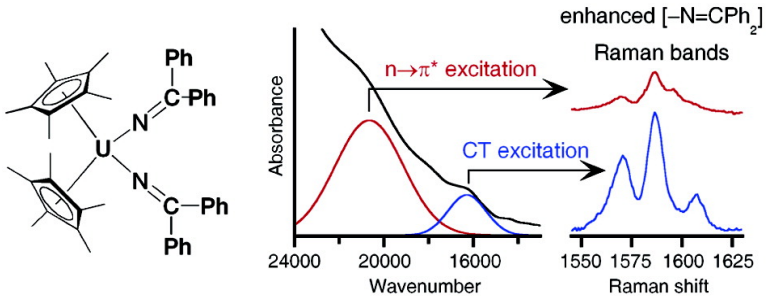

More About This Article

Additional resources and features associated with this article are available within the HTML version:

- Supporting Information
- Links to the 5 articles that cite this article, as of the time of this article download
- Access to high resolution figures
- Links to articles and content related to this article
- Copyright permission to reproduce figures and/or text from this article

View the Full Text HTML

J|A|C|S
ARTICLES
Published on Web 12/17/2004

Molecular Spectroscopy of Uranium(IV) Bis(ketimido) Complexes. Rare Observation of Resonance-Enhanced Raman Scattering from Organoactinide Complexes and Evidence for Broken-Symmetry Excited States

Ryan E. Da Re, Kimberly C. Jantunen, Jeffrey T. Golden, Jaqueline L. Kiplinger,* and David E. Morris*

Contribution from the Chemistry Division and the Glenn T. Seaborg Institute for Transactinium Science, Los Alamos National Laboratory, Los Alamos, New Mexico 87545

Received September 17, 2004; E-mail: kiplinger@lanl.gov; demorris@lanl.gov

Abstract: Electronic absorption and resonance-enhanced Raman spectra for ketimido (azavinylidene) complexes of tetravalent uranium, $(C_5Me_5)_2U[-N{=}C(Ph)(R)]_2$ (R = Ph, Me, and CH_2Ph), have been recorded. The absorption spectra exhibit four broad bands between 13 000 and 24 000 cm^{-1}. The highest-energy band is assigned to the ketimido-localized $p_\perp(N)\rightarrow\pi^*(N{=}C)$ transition based on comparison to the spectra of $(C_5H_5)_2Zr[-N{=}CPh_2]_2$ and $(C_5Me_5)_2Th[-N{=}CPh_2]_2$. Upon excitation into any of these four absorption bands, the $(C_5Me_5)_2U[-N{=}C(Ph)(R)]_2$ complexes exhibit resonance enhancement for several Raman bands attributable to vibrations of the ketimido ligands. Raman bands for both the symmetric and nominally asymmetric N=C stretching bands are resonantly enhanced upon excitation into the $p_\perp(N)\rightarrow\pi^*$-(N=C) absorption bands, indicating that the excited state is localized on a single ketimido ligand. Raman excitation profiles for $(C_5Me_5)_2U[-N{=}CPh_2]_2$ confirm that at least one of the lower-energy electronic absorption bands ($E_{max} \sim 16300$ cm^{-1}) is a charge-transfer transition between the U(IV) center and the ketimido ligand(s). The observations of both charge-transfer transitions and resonance enhancement of Raman vibrational bands are exceedingly rare for tetravalent actinide complexes and reflect the strong bonding interactions between the uranium 5f/6d orbitals and those on the ketimido ligands.

Introduction

Electronic states derived from the interactions between metals and ligands, for example, charge-transfer (CT) electronic excited states, and the typical spectroscopic manifestations of such states, including vibronically structured absorption and emission bands and/or resonance enhancement for Raman vibrational bands, are familiar aspects of transition-metal chemistry. For example, the $d(Ru)\rightarrow\pi^*(bpy)$ metal-to-ligand charge-transfer (MLCT) excited state of $[Ru(bpy)_3]^{2+}$ has enjoyed considerable attention over the past 30 years due to its relevance to important phenomena such as broken symmetry excited states and photoinduced electron and energy transfer.[1] Spectroscopic evidence for ligand-to-metal charge-transfer (LMCT) excited states is most commonly observed for homoleptic oxo and halide complexes such as $[MnO_4]^-$ and $[IrCl_6]^{2-}$.[2]

Interest in the LMCT excited states of organometallic systems, and particularly those that are emissive in solutions or glasses, has increased in recent years.[3,4] Notable examples include metallocene complexes such as $(C_5H_5)_2Ti[-N{=}C{=}S]_2$ (**1**)[3] and imido complexes such as *cis,mer*-$M(\equiv NAr)X_3L_2$ (M = Nb, Ta; L = N and O σ-donating ligand; X = halide) (**2**)[4] which possess d^0 ground-state electronic configurations (Chart 1). Many of these complexes exhibit long-lived emission from low-energy LMCT excited states in conventional solvents.

In contrast, there is a very limited range of actinide complexes for which spectroscopic evidence for charge-transfer excited states has been reported. The overwhelming majority of actinide systems having this spectral feature are coordination complexes of the trans dioxo (actinyl) cations, $[AnO_2]^{n+}$, for which the actinide-oxo ligand multiple bonding introduces low-lying excited states of ligand-to-metal charge-transfer character.[5] The paucity of other examples of charge-transfer excited states in actinide complexes is largely due to the fact that the charge-transfer excited-state properties of nonactinyl actinide complexes, and in particular, those of organoactinide complexes, remain largely unexplored. The recent growth of organoactinide chemistry, and in particular the incorporation of ligands having rich electronic properties of their own, has opened the door to identifying and developing many new systems that possess novel electronic and magnetic properties. Spectroscopic studies of these systems that focus on molecular excited-state properties (e.g., charge-transfer states) promise to further our understanding

(1) Balzani, V.; Juris, A.; Venturi, M. *Chem. Rev.* **1996**, *96*, 759−833.
(2) Lever, A. B. P. *Inorganic Electronic Spectroscopy*; Elsevier: Amsterdam, 1984; Vol. 33.
(3) Patrick, E. L.; Ray, C. J.; Meyer, G. D.; Ortiz, T. P.; Marshall, J. A.; Brozik, J. A.; Summers, M. A.; Kenney, J. W. III *J. Am. Chem. Soc.* **2003**, *125*, 5461−5470.
(4) Heinselman, K. S.; Hopkins, M. D. *J. Am. Chem. Soc.* **1995**, *117*, 12340−12341.
(5) See, for example; (a) Denning, R. G.; Snellgrove, T. R.; Woodwark, D. R. *Mol. Phys.* **1976**, *32*, 419−442. (b) Denning, R. G. *Struct. Bonding* **1992**, *79*, 215−276.

10.1021/ja044315g CCC: $30.25

Chart 1. Examples of Complexes Having Emissive LMCT Excited States

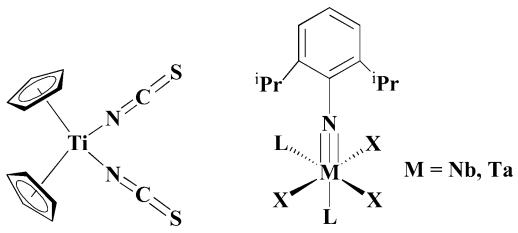

1 **2**

Chart 2. Actinide Ketimido Complexes under Investigation in This Work

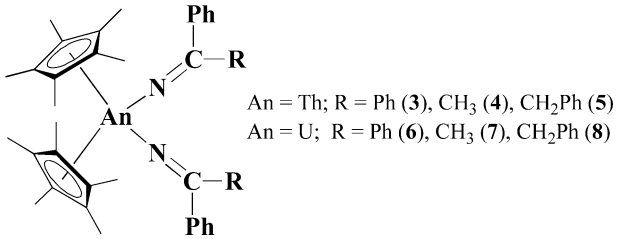

Chart 3. Comparison of Metrical Parameters for $(C_5Me_5)_2U[-N{=}CPh_2]_2$ (**6**) and $(C_5H_5)_2Zr[-N{=}CPh_2]_2$ (**9**)

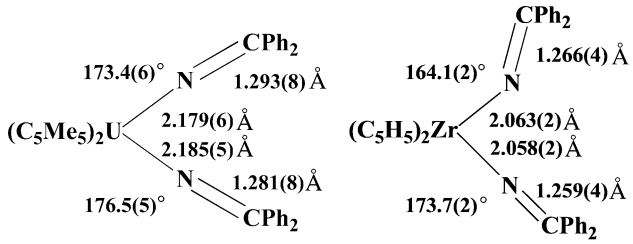

6 **9**

of f-element electronic structure and actinide-ligand bonding schemes.

Recently we reported a series of organometallic actinide ketimido complexes of the general form $(C_5Me_5)_2An[-N{=}C(Ph)(R)]_2$ (An = Th; Ph = C_6H_5, R = Ph (**3**), CH_3 (**4**), CH_2Ph (**5**): An = U; R = Ph (**6**), CH_3 (**7**), CH_2Ph (**8**)) that exhibit structural and spectroscopic evidence for unusually strong actinide-ligand bonding (Chart 2).[6,7] Notably, the anomalously large intensities in the f−f electronic transitions for the U(IV) complexes suggest that the f orbitals are directly involved in bonding to the ketimido ligands.[7] These complexes possess nearly linear An-N=C bonding for both [−N=C(Ph)(R)] ketimido ligands (e.g., ∠(U−N=C) = 173.4(6)° and 176.5(5)° for $(C_5Me_5)_2U[-N{=}CPh_2]_2$ (**6**), Chart 3). This is in contrast to the structurally related transition-metal complexes, $(C_5H_5)_2Ti[-N{=}C{=}S]_2$ (**1**)[3] and $(C_5H_5)_2Zr[-N{=}CPh_2]_2$ (**9**).[8,9] For example, $(C_5H_5)_2Zr[-N{=}CPh_2]_2$ (**9**) exhibits one nearly linear and one bent M−N=C linkage (e.g., ∠(Zr−N=C) = 173.7(2)° and 164.1(2)°, Chart 3).[8,9] Moreover, the An−N bond lengths in the $(C_5Me_5)_2An[-N{=}C(Ph)(R)]_2$ complexes (e.g., d(U−N) = 2.179(6) and 2.185(5) Å for $(C_5Me_5)_2U[-N{=}CPh_2]_2$ (**6**)) are intermediate between those typically observed for U(IV) bis(amido) complexes (e.g., d(U−N) = 2.267(6) Å for $(C_5Me_5)_2U[-NH(2,6\text{-}(CH_3)_2C_6H_3)]_2$)[10] and those for U(IV) mono(imido) complexes (e.g., d(U=N) = 1.952(12) Å for $(C_5Me_5)_2U[{=}N\text{-}2,4,6\text{-}{}^tBu_3C_6H_2)]$).[11] Together, these structural data suggest that the strength of the bonding interaction between the actinide and the ketimido ligands for the $(C_5Me_5)_2An[-N{=}C(Ph)(R)]_2$ complexes (**3**−**8**) exceeds that of actinide−amido complexes (bond order = 1).

The impact of these strong interactions on the electronic structures of the $(C_5Me_5)_2An[-N{=}C(Ph)(R)]_2$ complexes (**3**−**8**) is underscored by the novel molecular spectroscopic behavior they exhibit.[6,7] For example, they exhibit intense electronic absorption bands in the UV−visible spectral region that are not observed for An(IV) metallocene complexes having simple σ-donor ligands (e.g., $(C_5Me_5)_2An(CH_3)_2$; An = Th(IV), U(IV)).[7] This observation is particularly remarkable for the Th(IV) complexes since the formal $6d^05f^0$ ground-state electronic configuration typically gives rise to colorless complexes, whereas these thorium ketimido complexes (**3**−**5**) are iridescent yellow or orange.[6b,12] These $(C_5Me_5)_2Th[-N{=}C(Ph)(R)]_2$ complexes (**3**−**5**) also possess intense, vibronically structured visible emission spectra.[13] For the U(IV) complexes (**6**−**8**), no visible emission is observed, presumably because of efficient relaxation of the higher-lying excited states into the lower-energy states derived from the $5f^2$ configuration. However, coupling between the states responsible for these intense UV−visible absorption bands and the lower-energy intra-$5f^2$ states has been postulated to provide an intensity-stealing mechanism that enhances the intensities of the intra-$5f^2$ transition bands by an order of magnitude relative to those found for $(C_5Me_5)_2U(CH_3)_2$ and similar U(IV) metallocenes having only σ-donor ligands in the metallocene wedge.[7]

Our initial spectroscopic observations for the $(C_5Me_5)_2An[-N{=}C(Ph)(R)]_2$ complexes (**3**−**8**) suggested that these systems might possess rich molecular spectroscopic properties rivaling those seen in transition-metal systems, and prompted us to undertake more detailed investigations. Herein we report resonance-enhanced Raman vibrational spectra for the $(C_5Me_5)_2U[-N{=}C(Ph)(R)]_2$ complexes (**6**−**8**) obtained with excitation into the visible absorption bands. To the best of our knowledge, these actinide systems represent only the *second* example of nonactinyl complexes for which resonance enhancement of vibrational Raman bands has been observed. Additionally, this work represents the *first* nonactinyl example for which one of the resonant electronic transition is a bona fide charge-transfer transition. The only other nonactinyl actinide systems for which resonance-enhanced Raman data have been reported include uranocene $U(C_8H_8)_2$ and its methylated derivative, $U(1,3,5,7\text{-}(CH_3)_4\text{-}C_8H_4)_2$.[14] However, the resonant electronic transitions giving rise to the Raman spectra in these complexes

(6) (a) Kiplinger, J. L.; Morris, D. E.; Scott, B. L.; Burns, C. J. *Organometallics* **2002**, *21*, 3073−3075. (b) Jantunen, K. C.; Burns, C. J.; Castro-Rodriguez, I.; Da Re, R. E.; Golden, J. T.; Morris, D. E.; Scott, B. L.; Taw, F. L.; Kiplinger, J. L. *Organometallics* **2004**, *23*, 4682−4692.
(7) Morris, D. E.; Da Re, R. E.; Jantunen, K. C.; Castro-Rodriguez, I.; Kiplinger, J. L. *Organometallics* **2004**, *23*, 5142−5153.
(8) Erker, G.; Fromberg, W.; Kruger, C.; Raabe, E. *J. Am. Chem. Soc.* **1988**, *110*, 2400−2405.
(9) Zippel, T.; Arndt, P.; Ohff, A.; Spannenberg, A.; Kempe, R.; Rosenthal, U. *Organometallics* **1998**, *17*, 4429−4437.
(10) Straub, T.; Frank, W.; Reiss, G. J.; Eisen, M. S. *J. Chem. Soc., Dalton Trans.* **1996**, 2541−2546.
(11) Arney, D. S. J.; Burns, C. J. *J. Am. Chem. Soc.* **1995**, *117*, 9448−9460.
(12) The lack of metal-localized valence electrons for these Th(IV) complexes also establishes a strong analogy to the d^0 $(C_5H_5)_2M(L)_n$ transition-metal systems noted above.
(13) Clark, A. E.; Da Re, R. E.; Jantunen, K. C.; Morris, D. E.; Kiplinger, J. L.; Hay, P. J.; Martin, R. L. Manuscript in preparation.

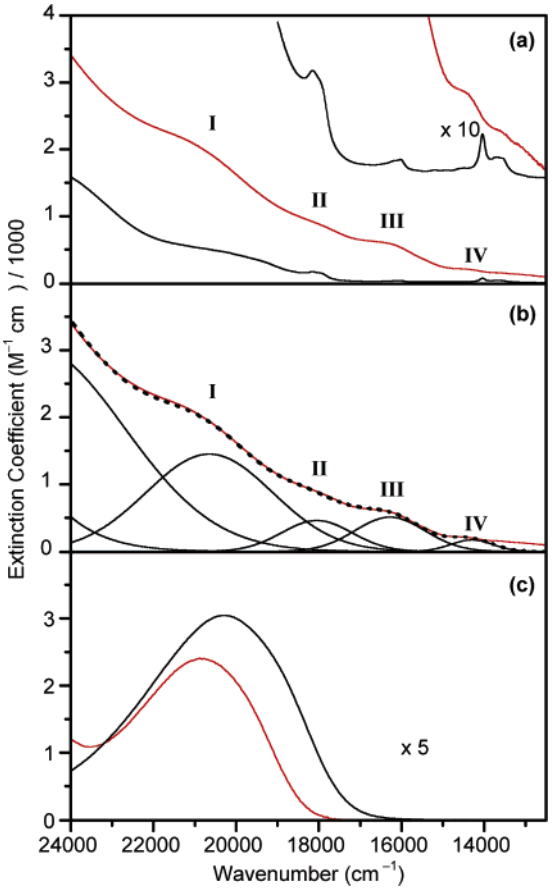

Figure 1. Electronic absorption spectra of $(C_5Me_5)_2An(L)_2$ complexes at 300 K: (a) $(C_5Me_5)_2U[-N{=}CPh_2]_2$ (**6**) (red) and $(C_5Me_5)_2U(Me)_2$ (black) in toluene; (b) deconvolution of the spectral envelope of $(C_5Me_5)_2U[-N{=}CPh_2]_2$ (**6**) into Gaussian bands; (c) $(C_5Me_5)_2Th[-N{=}CPh_2]_2$ (**3**) in toluene (red) and $(C_5H_5)_2Zr[-N{=}CPh_2]_2$ (**9**) (black) in 2-MeTHF. The expanded traces in panel (a) have been vertically offset for clarity.

were subsequently shown to be $5f^2 \rightarrow 5f^16d^1$ in character on the basis of a theoretical investigation of their low-energy excited states.[15]

Results and Discussion

The electronic absorption spectrum of $(C_5Me_5)_2U[-N{=}CPh_2]_2$ (**6**) at 300 K is characterized by several broad, overlapping absorption bands that span the entire UV−visible region.[7] These absorptions engender the complex with a dark brown-red color, which is in sharp contrast to the colors observed for other $(C_5Me_5)_2UL_2$ complexes in which L is a simple σ-donor ligand; for example, $(C_5Me_5)_2U(CH_3)_2$ is pale orange in color.[16] The darker color of the ketimido complex is largely due to the fact that it exhibits appreciable absorption ($\epsilon \sim 250-1000$) below 18000 cm^{-1} whereas $(C_5Me_5)_2U(CH_3)_2$ does not, as shown in Figure 1a. Moreover, the absorption intensity is considerably greater in the region above 18000 cm^{-1} for $(C_5Me_5)_2U[-N{=}CPh_2]_2$ than for $(C_5Me_5)_2U(CH_3)_2$. Deconvolution of the spectrum of $(C_5Me_5)_2U[-N{=}CPh_2]_2$ (**6**) into a sum of Gaussian bands (Figure 1b) reveals that a minimum of four broad absorptions contribute to the profile between 13 000 and 24 000 cm^{-1}, which we label I−IV in order of decreasing energy. The electronic absorption spectra of $(C_5Me_5)_2U[-N{=}C(Ph)(Me)]_2$ and $(C_5Me_5)_2U[-N{=}C(Ph)(CH_2Ph)]_2$ (**7** and **8**; not shown) are very similar to that of $(C_5Me_5)_2U[-N{=}CPh_2]_2$ in this region.[7]

Qualitative assignments for the absorption bands of $(C_5Me_5)_2U[-N{=}CPh_2]_2$ (**6**) are afforded by comparing and contrasting its spectrum with those of $(C_5Me_5)_2U(CH_3)_2$ and the related complexes $(C_5Me_5)_2Th[-N{=}CPh_2]_2$ (**3**) and $(C_5H_5)_2Zr[-N{=}CPh_2]_2$ (**9**). As shown in Figure 1c, the absorption spectra of $(C_5Me_5)_2Th[-N{=}CPh_2]_2$ and $(C_5H_5)_2Zr[-N{=}CPh_2]_2$ both exhibit a moderately intense absorption band near 21 000 cm^{-1} that carries similar intensity for both complexes. The remarkable insensitivity of the energy and intensity of this absorption band to the metal (Zr vs Th) and the modest oscillator strength of the electronic transition ($\epsilon \sim 500$) indicate an assignment to a spin-allowed but orbitally forbidden transition localized on the $[-N{=}CPh_2]$ ligands. The most plausible candidate for such an assignment is the $p_\perp(N) \rightarrow \pi^*(N{=}C)$ transition, where $p_\perp(N)$ refers to a nitrogen-based p orbital that lies in the (idealized) $N{=}C(C_{ipso})_2$ plane that is orthogonal to the $\pi/\pi^*(N{=}C)$ orbitals.[17] Importantly, the characteristics of these $n \rightarrow \pi^*$ bands compare very well with those of band I for $(C_5Me_5)_2U[-N{=}CPh_2]_2$ (Figure 1b), indicating that it too likely derives from an $n \rightarrow \pi^*$ transition. In contrast, bands II−IV have no counterparts in the spectra of $(C_5Me_5)_2Th[-N{=}CPh_2]_2$ (**3**) and $(C_5H_5)_2Zr[-N{=}CPh_2]_2$ (**9**), indicating that they cannot be attributed to transitions localized purely on the $[-N{=}CPh_2]$ ligands. Moreover, the absence of bands II−IV from the spectrum of $(C_5Me_5)_2U(CH_3)_2$ indicates that they cannot be attributed to charge-transfer transitions originating on the C_5Me_5 ligands. While it is likely that transitions within the $5f^2$ configuration give rise to weak (and presumably obscured) absorptions in this region as observed for $(C_5Me_5)_2U(CH_3)_2$ (Figure 1a), the intensity and broadness of each band in this spectral region are inconsistent with such an assignment. Thus, bands II−IV must correspond to either $5f^2 \rightarrow 5f^16d^1$ transitions or charge-transfer transitions involving the U(IV) center and the ketimido ligands, with the latter being the most probable assignment based on the electronic absorption data alone since $5f^2 \rightarrow 5f^16d^1$ transitions would also be observed in a similar spectral region for complexes such as $(C_5Me_5)_2U(CH_3)_2$. The resonance Raman data for $(C_5Me_5)_2U[-N{=}CPh_2]_2$ and its analogues (**6**−**8**) discussed below provide evidence to conclusively assign band III to a charge-transfer transition.

Resonance Raman spectroscopy is an invaluable tool for probing the changes in the vibrational potential-energy distribution that occur during an electronic transition between the ground state and the resonant excited state.[18] The intensities of Raman bands that correspond to modes which are vibronically active in the resonant excited state will be selectively enhanced, oftentimes by several orders of magnitude.[18] Thus, it is anticipated that Raman spectra obtained with excitation into

(14) (a) Dallinger, R. F.; Stein, P.; Spiro, T. G. *J. Am. Chem. Soc.* **1978**, *100*, 7865−7870. (b) Yamaguchi, S.; Spiro, T. G. *Chem. Phys. Lett.* **1984**, *110*, 209−213.
(15) (a) Chang, A. H. H.; Pitzer, R. M. *J. Am. Chem. Soc.* **1989**, *111*, 2500−2507. (b) Liu, W.; Dolg, M.; Fulde, P. *J. Chem. Phys.* **1997**, *107*, 3584−3591. (c) Li, J.; Bursten, B. E. *J. Am. Chem. Soc.* **1998**, *120*, 11456−11466.
(16) Fagan, P. J.; Manriquez, J. M.; Maatta, E. A.; Seyam, A. M.; Marks, T. J. *J. Am. Chem. Soc.* **1981**, *103*, 6650−6667.
(17) This assignment of ligand-based excitations, for which time-dependent density functional theory calculations have played a key role, is developed more fully in a forthcoming paper where theoretical and experimental studies of excited states of $(C_5Me_5)_2Th[-N{=}CPh_2]_2$ and $(C_5H_5)_2Zr[-N{=}CPh_2]_2$ are presented (ref 13).
(18) Clark, R. J. H.; Dines, T. J. *Angew. Chem., Int. Ed. Engl.* **1986**, *25*, 131−158.

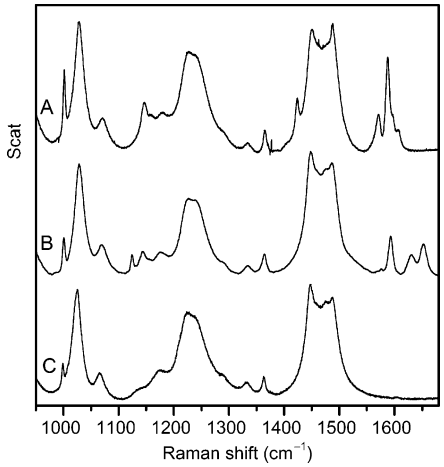

Figure 2. Resonance Raman spectra of ketimido complexes (10 mM in THF solution) at 300 K: (A) $(C_5Me_5)_2U[-N{=}CPh_2]_2$ (**6**) obtained with λ_{ex} = 514.5 nm (19436 cm^{-1}); (B) $(C_5H_5)_2Zr[-N{=}CPh_2]_2$ (**9**) obtained with λ_{ex} = 457.9 nm (21839 cm^{-1}); (C) neat THF obtained with λ_{ex} = 514.5 nm. The spectra have been vertically offset for clarity.

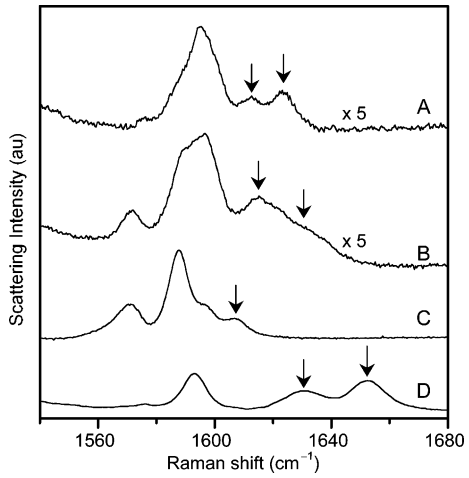

Figure 3. ν(CN) Raman bands of ketimido complexes: (A) $(C_5Me_5)_2U[-N{=}C(Ph)(Me)]_2$ (**7**) obtained with λ_{ex} = 514.5 nm (19436 cm^{-1}); (B) $(C_5Me_5)_2U[-N{=}C(Ph)(CH_2Ph)]_2$ (**8**) obtained with λ_{ex} = 514.5 nm; (C) $(C_5Me_5)_2U[-N{=}CPh_2]_2$ (**6**) obtained with λ_{ex} = 514.5 nm; (D) $(C_5H_5)_2Zr[-N{=}CPh_2]_2$ (**9**) obtained with λ_{ex} = 457.9 nm (21839 cm^{-1}). The spectra have been vertically offset for clarity. The arrows indicate the positions of the ν(CN) bands.

absorption bands involving $[-N{=}CPh_2]$ orbitals will exhibit selective enhancement for Raman bands associated with $[-N{=}CPh_2]$-localized and U−N vibrational modes. Raman vibrational spectra have been acquired under resonance excitation conditions for the $(C_5Me_5)_2U[-N{=}C(Ph)(R)]_2$ complexes (**6**−**8**) and $(C_5H_5)_2Zr[-N{=}CPh_2]_2$ (**9**) in THF solution. Representative spectral data are shown in Figures 2 and 3, and vibrational frequencies and relative scattering intensities are set out in Table 1. Notably, even at the low concentrations of complex (∼10 mM) present in each of the samples used to collect the spectra shown in Figure 2, the intensities of the Raman bands derived from the complexes under resonant excitation conditions are comparable to those corresponding to THF bands (∼12 M as a neat liquid). This observation indicates that the intensities of these Raman bands are resonance enhanced, and as expected for resonance enhancement, the intensities vary with excitation wavelength (vide infra). These observations are particularly noteworthy for the $(C_5Me_5)_2U[-N{=}C(Ph)(R)]_2$ complexes (**6**−**8**), because to our knowledge the only other nonactinyl actinide complexes for which such behavior has been reported are the organoactinide paradigm, uranocene $[U(C_8H_8)_2]$, and the methylated variant, $U(1,3,5,7\text{-}(CH_3)_4{-}C_8H_4)_2$.[14,19]

The resonance Raman spectrum of $(C_5H_5)_2Zr[-N{=}CPh_2]_2$ (**9**) obtained with excitation into its n→π* absorption band exhibits several bands above 1500 cm^{-1} that correspond to vibrations localized on the $[-N{=}CPh_2]$ ligands (Figure 3D). The pair of bands at 1652 and 1631 cm^{-1} are assigned to the nominal C=N stretching vibrations. The energies of these bands are in excellent agreement with those of the bands found at 1650 and 1630 cm^{-1} in the infrared spectrum of this compound.[8,20] The Raman spectrum of $(C_5H_5)_2Zr[-N{=}CPh_2]_2$ (**9**) in this region also exhibits a set of four bands at 1595, 1588, 1576, and 1569 cm^{-1} that are assigned to C−C stretching vibrations of the phenyl rings. The energies of the higher frequency C−C stretching vibrations in this set are in excellent agreement with those determined from the Raman spectrum of tetraphenylethylene (ν(CC, Ph) = 1595 and 1588 cm^{-1}); no counterparts to the 1576 and 1569 cm^{-1} bands were reported for tetraphenylethylene.[21] Notably, the enhancement of the $[-N{=}CPh_2]$ Raman bands with excitation into the n→π* absorption band is consistent with the orbital character of the n→π* transition in which there is a significant distortion in these ligand normal coordinates between the ground and excited states.

The resonance Raman spectra of the $(C_5Me_5)_2U[-N{=}C(Ph)(R)]_2$ complexes (**6**−**8**) are similar to that of $(C_5H_5)_2Zr[-N{=}CPh_2]_2$ (**9**) above 1500 cm^{-1} with the key difference being a significant shift to lower energy in the C=N stretching bands from those of $(C_5H_5)_2Zr[-N{=}CPh_2]_2$ (vide infra). Unlike the Raman spectrum of $(C_5H_5)_2Zr[-N{=}CPh_2]_2$, in which the C=N stretching bands are well separated from those corresponding to vibrations of the Ph groups (Figure 3D), the spectra of the $(C_5Me_5)_2U[-N{=}C(Ph)(R)]_2$ complexes (**6**−**8**; Figure 3A−C) exhibit a cluster of bands centered near 1600 cm^{-1} that correspond to vibrations localized on their respective $[-N{=}C(Ph)(R)]$ ligands. Importantly, the Raman spectrum of each $(C_5Me_5)_2U[-N{=}C(Ph)(R)]_2$ complex (**6**−**8**) exhibits four bands that are straightforwardly assigned to ν(CC, Ph) on the basis of comparison to the 1593, 1588, 1576, and 1569 cm^{-1} bands of $(C_5H_5)_2Zr[-N{=}CPh_2]_2$ (**9**; Table 1). The remaining bands, found above 1600 cm^{-1}, are assigned to C=N stretching vibrations.[20] As observed for $(C_5H_5)_2Zr[-N{=}CPh_2]_2$ (**9**), the Raman spectra of $(C_5Me_5)_2U[-N{=}C(Ph)(Me)]_2$ (**7**) and $(C_5Me_5)_2U[-N{=}C(Ph)(CH_2Ph)]_2$ (**8**) clearly exhibit two C=N stretching bands. Only one C=N stretching band is resolved in the Raman spectra of $(C_5Me_5)_2U[-N{=}CPh_2]_2$ (**6**). Notably, the average C=N stretching frequency for the $(C_5Me_5)_2U[-N{=}C(Ph)(R)]_2$ complexes (**6**−**8**) is downshifted by ca. 25 cm^{-1} from those of $(C_5H_5)_2Zr[-N{=}CPh_2]_2$ (**9**), suggesting that the C=N bonds of the uranium-ketimido complexes are comparatively weaker than those of the Zr-ketimido complex.

Previously it was suggested on the basis of the structural data for this class of compounds that the metal−ketimido interactions—and more specifically, the ketimido ligand N(2p) lone-pair

(19) Seyferth, D. *Organometallics* **2004**, *23*, 3562−3583.
(20) The N=C stretching vibrations should not be regarded as pure oscillators since they are most likely coupled to vibrations localized on the R groups. This will be particularly true for Ph-localized vibrations of the same symmetry with similar frequencies to the N=C stretching vibrations.
(21) Tahara, T.; Hamaguchi, H. *Chem. Phys. Lett.* **1994**, *217*, 369−374.

Table 1. Raman Shifts and Scattering Intensities for $(C_5Me_5)_2U[-N{=}C(Ph)(R)]_2$ (**6**−**8**) and $(C_5H_5)_2Zr[-N{=}CPh_2]_2$ (**9**) in THF Solution at 300 K[a]

$(C_5Me_5)_2U[-N{=}C(Ph)(R)]_2$[b]						$(C_5H_5)_2Zr[-N{=}CPh_2]_2$[c]		*Assignment*[d]
R = Ph		R = CH_2Ph		R = Me				
		1631	m	1623	m	1652[e]	s	ν (CN)
1605	m	1615	m	1612	m	1631[e]	s	ν (CN)
1595	m	1597	s	1596	s	1593	s	ν (CC), Ph
1586	s	1589	s	1588	m, sh	1588[f]	w, sh	ν (CC), Ph
1569	m	1572	m	1578	w	1576	w	ν (CC), Ph
1562[f]	w, sh					1569	vw	ν (CC), Ph
1486[g]	m	1488[g]	m					ν (CC), Ph
1444[g]	vw	1444[g]	vw					ν (CC), Ph
1423	m	1424	m	1423	m	1124[h]	m	ν (CC) + ν (C-Me), C_5Me_5[h]
1404[g]	vw	1404[g]	vw					ν (CC) + ν (C-Me), C_5Me_5
1384[g]	vw	1382[g]	vw					$\delta(CH_3)$, C_5Me_5
1368[g]	vw	1368[g]	vw					Ph
1246[g]	vw	1243[g]	vw					Ph
1146	m					1143	m	Ph
1026	w	1020	m					Ph
1001[g]	m	1000[g]	m	1000[g]	m	999[g]	m	Ph
733	w					734	w	Ph
						720	w	Ph
632	vw				vw	632	vw	Ph
622	vw					620	vw	Ph
614	w	614	vw	617	vw	615	w	Ph
590	vw	594	vw	592	vw			C_5Me_5
550	vw	555	vw	542	vw			C_5Me_5
						476	vw	Ph
		430	vw	425	vw	402	vw	Ph
382	w, b	381	vw, b	380	vw, b	348[i]	vw	ν (U-C_5Me_5)[i]
302	vw	300	vw	300	vw			Ph
232	vw	231	vw	232	vw			Ph
210	vw	210	vw	210	vw			
182	vw							

[a] Mode energies in cm^{-1}. Intensity legend: vw = very weak, w = weak, m = moderate, s = strong, b = broad, sh = shoulder. [b] λ_{ex} = 514.5 nm. [c] λ_{ex} = 457.9 nm. [d] Assignments of bands due to Ph-localized and C_5Me_5/C_5H_5 vibrations are taken from refs 21 and 23, respectively. [e] The corresponding bands in the infrared spectrum of $(C_5H_5)_2Zr[-N{=}CPh_2]_2$ are found at 1650 cm^{-1} (sh) and 1630 cm^{-1} (s) (see ref 8). [f] Identified by deconvolution. [g] Recorded in THF-d_8. [h] ν (CC), C_5H_5 for $(C_5H_5)_2Zr[-N{=}CPh_2]_2$. [i] Assignments based on ν (Zr−C_5H_5) for $(C_5H_5)_2Zr[-N{=}CPh_2]_2$.

π-bonding interactions with the U(IV) metal center—are stronger in the case of the $(C_5Me_5)_2U[-N{=}C(Ph)(R)]_2$ complexes (**6**−**8**) than for their transition-metal congeners, such as $(C_5H_5)_2Zr[-N{=}CPh_2]_2$ (**9**).[6,7] For example, the average C=N bond distance was found to be slightly longer (~0.02−0.03 Å) for the $(C_5Me_5)_2U[-N{=}C(Ph)(R)]_2$ complexes (**6**−**8**) than for $(C_5H_5)_2Zr[-N{=}CPh_2]_2$ (**9**). This notion is borne out by the C=N stretching frequency data reported here.

The observation of two C=N stretching bands in the resonance Raman spectra of the $(C_5Me_5)_2U[-N{=}C(Ph)(Me)]_2$ (**7**) and $(C_5Me_5)_2U[-N{=}C(Ph)(CH_2Ph)]_2$ (**8**) with λ_{ex} = 514.5 nm is rather surprising and merits additional discussion. In general, resonance enhancement for Raman vibrational bands under normal (i.e., Franck−Condon or so-called A-term) conditions is observed only for totally symmetric vibrations.[18,22] The crystal structure of $(C_5Me_5)_2U[-N{=}C(Ph)(CH_2Ph)]_2$ (**8**) indicates that, in the solid state, the U(IV) center resides on a plane of symmetry that renders the $[-N{=}C(Ph)(CH_2Ph)]$ ligands equivalent.[6b] Under this point symmetry, the in-phase C=N stretch (i.e., the mode in which both C=N bonds elongate/compress simultaneously) is totally symmetric whereas the out-of-phase C=N stretch is not. Thus, only the former is expected to be resonantly enhanced under normal (i.e., Franck−Condon) resonance conditions. Resonance enhancement for a second C=N stretching mode under this same intensity-generating mechanism is only possible if the molecular geometry is sufficiently reduced in the resonant excited-state such that both C=N stretches become totally symmetric vibrations. This condition, referred to as "broken symmetry", is easily satisfied if the n→π^* excited state is localized on one $[-N{=}C(Ph)(CH_2Ph)]$ ligand (e.g., the C=N bond of one ketimide ligand would be elongated in the excited state). The fact that both C=N stretching bands are resonantly enhanced for $(C_5Me_5)_2U[-N{=}C(Ph)(CH_2Ph)]_2$ (**8**) suggests that this is indeed the case. Conversely, the structural data for $(C_5H_5)_2Zr[-N{=}CPh_2]_2$ (**9**), and in particular, the ∠(Zr−N=C) values, suggest that the Zr−N=C linkages are already symmetry inequivalent in the ground state (d(Zr−N) = 2.058(2) Å and 2.063(2) Å; d(N−C) = 1.259(4) Å and 1.266(4) Å; ∠(Zr−N=C) = 164.1(2)° and 173.7(2)°)[9] (Chart 3). The fact that both C=N stretching bands are resonantly enhanced in the spectrum of $(C_5H_5)_2Zr[-N{=}CPh_2]_2$ (**9**) likely reflects this inequivalence of the $[-N{=}CPh_2]$ ligands, which renders both C=N stretching vibrations totally symmetric. It should be noted that a C_{2v}-symmetric structure for $(C_5H_5)_2Zr[-N{=}CPh_2]_2$ (**9**) in room-temperature solution has been inferred from the NMR-spectroscopic data for this compound,[9] although the shorter time scale for the resonance Raman scattering process enables discrimination between structures that are otherwise time averaged in the NMR experiment.

(22) It should be noted that Raman bands for nontotally symmetric vibrations can gain intensity if the resonant excited state is vibronically coupled to a second excited state (B-term enhancement, ref 18). Because the extent to which B-term scattering is operative is inversely proportional to the energetic separation between the coupled states, it is usually much less important than A-term scattering. This is particularly true for excited states in which the distortions are large, as expected for the resonant excited states under discussion in this work.

Two discrete C═N modes might also be expected in the resonance Raman spectrum of $(C_5Me_5)_2U[-N{=}CPh_2]_2$ (**6**) under a broken-symmetry excited-state condition. We were not able to identify two modes in our spectral data for $(C_5Me_5)_2U[-N{=}CPh_2]_2$ (**6**). However, we cannot preclude the existence of two very closely spaced bands in our spectra that simply cannot be resolved under our experimental conditions.

The proposed localization of the n→π* excited state on a single [−N═C(Ph)(R)] ligand for the $(C_5Me_5)_2U[-N{=}C(Ph)(R)]_2$ complexes (**7**,**8**) can be contrasted with the behavior reported recently for the structurally related complex $(C_5H_5)_2Ti[-N{=}C{=}S]_2$ (**1**). For this titanocene complex, the lowest-energy excited states are delocalized across both [−N═C═S] ligands.[3] Specifically, it was observed that the relative intensities of the symmetric and asymmetric C═N stretching bands in the infrared spectrum of $(C_5H_5)_2Ti[-N{=}C{=}S]_2$ (**1**) are largely preserved for the lowest-energy $\pi(-N{=}C{=}S)$→d LMCT excited state, from which it was concluded that symmetry equivalence of the [−N═C═S] ligands is retained in the excited state. Moreover, several theoretical models of this excited state indicate that the LMCT transition generates a hole in a molecular orbital formed from a linear combination of π-symmetry orbitals localized on both [−N═C═S] ligands. While it is plausible based solely on symmetry considerations that the n→π* transition of the $(C_5Me_5)_2U[-N{=}C(Ph)(R)]_2$ complexes (**6**−**8**) originates in a molecular orbital that is delocalized across both [−N═C(Ph)(R)] ligands, the resonance Raman data—and specifically, the observation of symmetric and nominally asymmetric C═N stretching bands—strongly suggest that the excited electron (and presumably the corresponding hole) are localized on one [−N═C(Ph)(R)] ligand. A detailed theoretical investigation into the nature of the n→π* excited for the related complexes $(C_5Me_5)_2Th[-N{=}CPh_2]_2$ (**3**−**5**) will be discussed in a forthcoming paper.[13]

The resonance Raman spectra of $(C_5H_5)_2Zr[-N{=}CPh_2]_2$ (**9**) and the $(C_5Me_5)_2U[-N{=}C(Ph)(R)]_2$ complexes (**6**−**8**) are similar below 1500 cm^{-1}, exhibiting a wealth of vibrational bands that, for the most part, are readily assigned to vibrations of their cyclopentadienyl and ketimido ligands. Assignments for these ligand-localized vibrations (Table 1) are based on comparison to the Raman spectra of tetraphenylethylene[21] and several $(C_5R_5)ML_3$ complexes (R = H, Me; M = Mn, Re; L = O, CO).[23] Importantly, the frequencies for these Raman bands show a high degree of correlation from complex to complex, which simplifies the task of identifying Raman bands attributable to metal−ligand vibrations. In particular, the resonance Raman spectrum of each $(C_5Me_5)_2U[-N{=}C(Ph)(R)]_2$ complex (**6**−**8**) exhibits a weak band near 380 cm^{-1} that is not observed in the spectrum of $(C_5H_5)_2Zr[-N{=}CPh_2]_2$ (**9**) and has not been identified as a C_5Me_5 vibration, suggesting an assignment to a metal−ligand vibration. While it is impossible on the basis of existing data to distinguish between the assignment as ν(U−C_5Me_5) versus ν(U−N), we note that the narrow Raman-shift range defined by these bands (380−382 cm^{-1}) does not track with the much broader range of C═N stretching frequencies (1605−1631 cm^{-1}) found for these complexes, suggesting that assignment to ν(U−C_5Me_5) rather than ν(U−N) is more likely. Likewise, the 348 cm^{-1} Raman band of $(C_5H_5)_2Zr[-N{=}CPh_2]_2$ has no counterpart in the spectra of the $(C_5Me_5)_2U[-N{=}C(Ph)(R)]_2$ complexes, and is tentatively assigned to $\nu(Zr-C_5H_5)$. Notably, these putative M−C_5R_5 stretching frequencies agree well with those reported for several $(C_5R_5)ML_3$ complexes,[23] providing added support for these assignments.

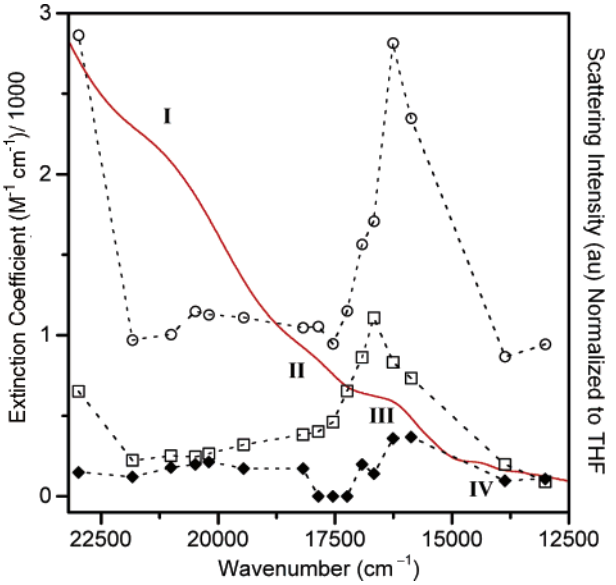

Figure 4. Raman excitation profiles for the 1605 (□), 1586 (○), and 1485 cm^{-1} (◆) vibrational modes of $(C_5Me_5)_2U[-N{=}CPh_2]_2$ (**6**) overlaid with its electronic absorption spectrum (red). The intensities of the $(C_5Me_5)_2U[-N{=}CPh_2]_2$ Raman bands are referenced to the intensity of the 1448 cm^{-1} band of THF. The dashed lines connecting data points have been added to assist in following the trends for the individual vibrational modes.

A detailed investigation of the wavelength dependence of the resonance enhancement effect observed for the Raman bands of $(C_5Me_5)_2U[-N{=}CPh_2]_2$ (**6**) was also undertaken to assist in a more detailed analysis and assignment of its electronic absorption spectrum. Raman excitation profiles for several Raman bands of $(C_5Me_5)_2U[-N{=}CPh_2]_2$ were determined, and those of the 1605 cm^{-1}, 1586 cm^{-1}, and 1485 cm^{-1} bands are shown in Figure 4 overlaid with the absorption spectrum of $(C_5Me_5)_2U[-N{=}CPh_2]_2$.[24] The available laser excitation wavelengths provide good coverage of bands I and III. The variation in the intensities of the Raman bands of $(C_5Me_5)_2U[-N{=}CPh_2]_2$ with excitation wavelength is quite pronounced in the vicinity of band III. As noted above, the fact that the [−N═CPh_2] Raman bands are enhanced with excitation into band I is consistent with the orbital character of the n→π* transition. The resonance enhancement of these same Raman bands with excitation into band III suggests that the corresponding electronic transition also involves [−N═CPh_2] orbitals.

The Raman excitation profile data provide definitive evidence that the distortions in the normal coordinates associated with the ketimido ligands are much greater in resonance with band III than with band I. Since band I has been assigned to an n→π* transition localized on a single ketimido ligand on the basis of both electronic spectral comparisons and resonance Raman data,

(23) Bencze, É.; Mink, J.; Németh, C.; Herrmann, W. A.; Lokshin, B. V.; Kühn, F. E. *J. Organomet. Chem.* **2002**, *642*, 246−258.

(24) Note that the excitation profiles shown in Figure 4 for the 1605 and 1586 cm^{-1} Raman bands maximize at λ_{ex} = 600 and 615 nm, respectively. While this may be an indication that the excitation profiles are structured in this region, we cannot exclude the possibility that both profiles maximize at an excitation wavelength between 600 and 615 nm, which is not represented in Figure 4. Raman excitation profiles for the 1569 and 1562 cm^{-1} [−N═CPh_2] Raman bands qualitatively track with that of the 1586 cm^{-1} band, whereas the excitation profile for the 1595 cm^{-1} band tracks with that of 1605 cm^{-1} band.

the implication is that the assignment for band III must provide for an even greater set of normal coordinate distortions on the ketimido ligands between the ground and excited electronic states. As noted above, probable assignments for band III are to either a $5f^2 \rightarrow 5f^16d^1$ transition or a charge-transfer transition. For the $U(C_8H_8)_2$ system, the observation of resonance enhancement in only two vibrational modes, one of which is the 211 cm^{-1} $U-(C_8H_8)$ totally symmetric stretch,[14] is entirely consistent with the subsequent theoretical prediction that the low-energy resonant electronic states are $5f^2 \rightarrow 5f^16d^1$ in character.[15] The $U-(C_8H_8)$ ring stretch would be expected to be perturbed by a change in the metal-localized electron density between 5f and 6d orbitals. In contrast, for the $(C_5Me_5)_2U[-N=C(Ph)(R)]_2$ complexes (**6**−**8**) studied here, the observation of apparent large distortions along *many* normal coordinates localized on the ketimido ligand framework is inconsistent with expectations for a predominantly metal-localized electronic transition. Thus, a charge-transfer assignment for band III is conclusively supported by the Raman excitation profile data.[25] Unfortunately, neither electronic nor resonance Raman data for $(C_5Me_5)_2U[-N=CPh_2]_2$ (**6**) allow us to determine the direction of the charge transfer in the band-III transition (i.e., ligand-to-metal or metal-to-ligand). Nonetheless, the low oscillator strength ($\epsilon \sim 500$) does indicate that the metal-based orbitals involved in this transition are principally 5f in character rather than 6d, since the greater radial extent of the 6d orbitals would be expected to lead to greater intensity in the charge-transfer transition as observed in d transition-metal systems.

The intensities of the $[-N=CPh_2]$ Raman bands increase sharply with $\lambda_{ex} = 435$ nm, which is well above the maximum of the $n \rightarrow \pi^*$ band. This excitation wavelength is in resonance with one or more intense, higher-energy absorption bands, some of which presumably correspond to $\pi \rightarrow \pi^*$-type transitions of the $[-N=CPh_2]$ ligands. As expected, the intensities of the $[-N=CPh_2]$ Raman bands typically increase as λ_{ex} is shifted toward the maxima of these intense absorptions.

The enhancement of Raman bands corresponding to $\nu(U-C_5Me_5)$ and C_5Me_5-localized vibrations under bands I and III deserves comment. The fact that these vibrations are in resonance with the $n \rightarrow \pi^*$ and charge-transfer transitions (bands I and III) suggests that the corresponding electronic transitions perturb the electron density at the metal center sufficiently to invoke distortions along the $U-C_5Me_5$ and C_5Me_5-localized normal coordinates. The fact that the observed enhancement for these bands is weak certainly suggests that the effect is indirect. It should be noted that the present data do not allow us to exclude the possibility that the enhancement for these Raman bands is actually derived from the preresonance Raman effect with a higher-energy transition, such as a C_5Me_5-localized $\pi \rightarrow \pi^*$ or a LMCT transition originating in the C_5Me_5 π-orbitals, both of which should perturb $U-C_5Me_5$ and internal C_5Me_5 normal coordinates.

(25) The fact that the distortions are larger (hence the enhanced Raman intensities are greater) for the CT state is consistent with the orbital characters of the CT versus the $n \rightarrow \pi^*$ excited states. Removal of an electron from $p_\perp(N)$ reduces in-plane C−N π-symmetry antibonding interactions whereas population of $\pi^*(NC)$ increases out-of-plane C−N π-symmetry antibonding interactions. Thus, the net change in C−N bond order in the $n \rightarrow \pi^*$ excited state is inferred to be small. Conversely, removal of an electron from $\pi(CN)$ (as in a LMCT transition) or population of $\pi^*(CN)$ (as in a MLCT transition) reduces the C−N bond order by 0.5. Thus, distortions along $[N=CPh_2]$ coordinates are anticipated to be larger for LMCT and MLCT transitions than inferred for the $n \rightarrow \pi^*$ transition.

Summary

The spectroscopy of most traditional actinide coordination compounds and organoactinide complexes possessing only σ-donor ligands is dominated by metal-based electronic transitions derived from f−f and f−d states and vibrational transitions (infrared and Raman) having normal intensity-generating mechanisms. In contrast, the $(C_5Me_5)_2U[-N=C(Ph)(R)]_2$ ketimido complexes of U(IV) under investigation in this report exhibit novel molecular spectroscopic behavior including charge-transfer excited states and enhancement in the Raman vibrational spectra derived from resonant excitation with both charge-transfer and ligand-localized excited electronic states. Such behavior is a fairly common aspect of transition-metal coordination and organometallic chemistry. However, these uranium ketimido complexes are the first examples of tetravalent actinides to exhibit such rich molecular spectroscopic behavior. This novel behavior for the uranium ketimido complexes is attributed in large measure to the presence of energetically accessible orbitals localized on the ketimido ligands that (1) are able to interact with the metal center in both σ- and π-donor modes and (2) give rise to absorption bands through the visible region of the absorption spectrum. Notably, these ketimido systems are the first tetravalent actinide systems since the discovery and spectroscopic investigation of uranocene $[U(C_8H_8)_2]$ for which resonance Raman spectra have been reported. Importantly, the resonance Raman data for $(C_5Me_5)_2U[-N=CPh_2]_2$ afford an unequivocal assignment of its electronic absorption band centered at 16300 cm^{-1} (band III) to a charge-transfer transition between orbitals localized on the ketimido ligands and the U(IV) center.

Experimental Section

General Procedures and Materials. Samples for electronic and Raman spectroscopy were prepared under a nitrogen atmosphere using a recirculating Vacuum Atmospheres Model HE-553-2 inert atmosphere (N_2 or He) drybox with a MO-40-2 Dri-Train, or standard Schlenk and high vacuum line techniques. Glassware was dried overnight at 150 °C before use. Anhydrous toluene, tetrahydrofuran, ether, and benzene (Aldrich) were passed through a column of activated alumina (A2, 12 × 32, Purify) under nitrogen and stored over activated 4 Å molecular sieves prior to use. The reagents $(C_5H_5)ZrCl_2$ (Strem), $Ph_2C=NH$ (Aldrich), and $LiN(SiMe_3)_2$ (Aldrich) were used as received. The compounds $(C_5Me_5)_2U[-N=CPh_2]_2$ (**6**),[6] $(C_5Me_5)_2U[-N=C(Ph)(Me)]_2$ (**7**),[6b] $(C_5Me_5)_2U[-N=C(Ph)(CH_2Ph)]_2$ (**8**),[6b] $(C_5Me_5)_2U(Me)_2$,[16] and $(C_5Me_5)_2Th[-N=CPh_2]_2$ (**3**),[6b] were prepared using published procedures. The previously reported[9] complex $(C_5H_5)_2Zr[-N=CPh_2]_2$ (**9**) was prepared using a modified procedure as given below.

Synthesis of $(C_5H_5)_2Zr[-N=CPh_2]_2$ (9). A solution of $Ph_2C=NH$ (0.683 g, 3.76 mmol) in ether (15 mL) was treated with small portions (ca. 60 mg x 10) of $LiN(SiMe_3)_2$ (0.598 g, 3.58 mmol) at −35 °C. The resulting red solution was warmed to room temperature with stirring. The red solution was then added in portions (ca. 1 mL x 15) to $(C_5H_5)_2ZrCl_2$ (1.00 g, 3.42 mmol) in ether (45 mL). The reaction mixture was stirred for 16 h at ambient temperature. The resulting bright red solution was filtered through a 1 cm pad of Celite to remove lithium salts and the filter washed with toluene until the washings were colorless. Volatile materials were then removed from the filtrate in vacuo. The residue was then dissolved in a solution of benzene and toluene (15 mL:15 mL). This solution was filtered through a 1 cm pad of Celite and the filter media washed with toluene until the washings were colorless. Volatile materials were removed from the filtrate in vacuo. The resulting bright red residue was dissolved in a minimum volume of toluene and

cooled to −35 °C for recrystallization. The product, $(C_5H_5)_2Zr$ [−N═$CPh_2]_2$ (**9**), was isolated on a medium porosity fritted funnel (1.65 g, 80%).

Spectroscopy. Resonance Raman spectra of samples in THF (or THF-d_8) sealed in NMR tubes (Wilmad, Medium-walled tubes) were obtained using excitation (λ_{ex}) from a Spectra Physics 2045 Ar-ion laser; an Ar-ion-pumped Coherent Radiation 599 dye laser charged with trans-stilbene, Rhodamine-6G, or Rhodamine-110 dyes; or an Ar-ion-pumped Spectra Physics 3900 Ti:sapphire laser. For $\lambda_{ex} \leq 560$ nm, scattered light was collected and directed into a Jobin Yvon HR640 spectrometer operated as either a single-stage or a triple-stage spectrograph equipped with an 1800 grooves/mm grating in the final stage; the single-stage spectrograph requires that the scattered light be passed through either a holographic notch filter (Kaiser) or an appropriate long-pass filter to reduce contributions from Rayleigh scattering. For $\lambda_{ex} \geq 570$ nm, scattered light was collected and directed into a Spex Industries 1877 triple-stage spectrograph equipped with 1800 grooves/ mm gratings. Typical resolution for both spectrometers is 2−5 cm^{-1}. For all excitation wavelengths, scattering intensities were recorded using a liquid-nitrogen cooled CCD detector (Princeton Instruments). A polarization scrambler was placed at the entrance slit of the spectrograph to minimize distortions in the observed scattering intensities due to wavelength-dependent instrument response to polarized light. Typical excitation powers and integration times were 20−50 mW and 15−120 min, respectively. Raman shifts were calibrated against an external reference of 4-acetamidophenol,[26] and spectra were corrected by subtraction of a spectral baseline obtained with a spline-fitting procedure.[27] The dispersioncharacteristics of our instrumentation typically require the acquisition and concatenation of several spectral windows to encompass the entire Raman shift range from ∼150−1700 cm^{-1} (e.g., two windows are required for 457.9 nm excitation and five are required 770 nm excitation); windows were selected such that adjacent windows contained sufficient overlap of Raman bands to derive a continuous trace. Peak positions were determined by fitting band profiles. Electronic absorption spectra were recorded using a Perkin-Elmer Lambda 19 spectrophotometer. Samples were contained in quartz cuvettes modified for use with air-sensitive compounds.

Acknowledgment. Support for this research was provided by the United States Department of Energy, Office of Science, Office of Basic Energy Science, under the auspices of the Heavy Element Chemistry Program and the Los Alamos National Laboratory's Laboratory Directed Research and Development Office. K.C.J. and R.E.D acknowledge fellowship support from the G. T. Seaborg Institute for Transactinium Science at Los Alamos. We are grateful to Dr. Robert Donohoe (LANL) for technical assistance and helpful discussions. This research was performed at Los Alamos National Laboratory under contract with the University of California (Contract No. W-7405-ENG-36).

JA044315G

(26) Raman shift data for 4-acetamidophenol (Tylenol) can be found at: http://www.chemistry.ohio-state.edu/∼rmccreer/freqcorr/images/ tylenol.html.
(27) Bailey, J. A. Private communication.